

A 10 μm Pitch Interconnection Technology using Micro Tube Insertion into Al-Cu for 3D Applications

B. Goubault de Brugière, F. Marion, M. Fendler, V. Mandrillon, A. Hazotte*, M. Volpert, H. Ribot
CEA – LETI, MINATEC

17, rue des Martyrs – 38054 Grenoble Cedex 9, France

* LEM3 –CNRS/UPV-M, Ile du Saulcy, Metz, France

baptiste.goubault@cea.fr, +33 (0) 4 38 78 13 38

Abstract

Future 3-D applications require a very low pitch for inter-strata vertical interconnection. The last International Technology Roadmap for Semiconductors (ITRS) assessment for vertical interconnection predicts a need for decreasing the interconnection pitch to 10 μm [1]. The room-temperature insertion technology has been proposed and developed using micro tubes as inserts [3] to address many assembling difficulties of industrial process.

In the present work, we study the mechanical and electrical behavior of a single micro tube insertion into Al-0.5Cu pads. A modified nanoindenter with a very accurate load and displacement control is used, coupled with an electrical measurement device to qualify the insertion process.

Finally, the best Die To Wafer (D2W) parameters are determined thanks to a composed experimental design.

Introduction

State of the art interconnection technologies such as reflow soldering, thermo-compression and Direct Bond Interconnect (DBI), usually present limitations caused by planarity defects, high process loads and temperature, or exhibit low hybridization speeds. As an example, below 10 μm pitch planarity defects and unconnected bumps cannot be balanced when using reflow soldering approach because of the increasing number of interconnections and of the smaller size of bumps. Then, some local overpressure or parallelism issues can be induced when thermo-compression technique is used to compensate non-planarity. Finally, a very high surface planarity and roughness is mandatory when using low speed DBI integration. Some original bonding technologies have been proposed such as insertion technics [3], [8], [9].

The room-temperature insertion technology illustrated in figure 1, has been developed using micro tubes as inserts by D. Saint-Patrice et al. [3]. Hard micro tubes are used to penetrate into a softer material in order to establish a reliable electromechanical contact. As summarized in table 1, this technique allows reaching a 10 μm interconnection pitch and has been chosen in order to reduce the insertion load, to compensate planarity and uniformity defects and to carry out reliable integration without the use of flux. Indeed, the micro tube insertion breaks this oxide layer and the electrical and mechanical contacts are established. Moreover, as it is a room temperature process, all the issues due to different coefficients of thermal expansion (CTE) are avoided. However, in order to meet industrial requirements it is mandatory to achieve electromechanical characterization of the micro tube insertion and to reduce the D2W integration

time. That is why it is necessary to make an exhaustive mechanical characterization of the single micro tube insertion coupled with electrical measurements.

10 μm pitch	Yes?
Low assembling force	Yes
Planarity compensation	Yes?
Room temperature	Yes
No flux used	Yes
Low D2W bonding time	Yes?
Wafer To Wafer integration	No?

Table 1: Micro tube technic capabilities

The main objective of this work is to determine the best insertion conditions to decrease the final assembly cost and to reduce the pick and place process time as much as possible.

The present paper focuses on the mechanics of the micro tube insertion into Al-0.5Cu pads. This alloy is one of the most common materials used for microelectronic applications. For that purpose, we use a nanoindenter to analyze the insertion process and then add an electrical measurement device to characterize the evolution of the electrical contact during the insertion time. Finally, a composed experimental design of D2W hybridizations with more than 180 experiments is followed. These assemblies made with more than 95000 interconnections and with a 10 μm interconnection pitch are mechanically and electrically tested to validate our concept.

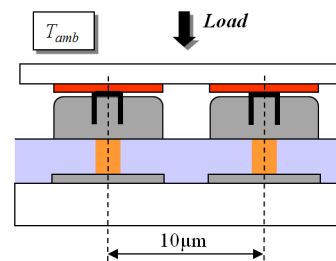


Fig. 1: Schematic drawing of the insertion flip-chip technique

1. Single micro tube insertion

In this part, we focus on the single micro tube insertion behavior into Al-Cu pads. First, mechanical insertion parameters of a single micro tube are determined. Then, the evolution of the electrical contact is characterized and related to the mechanical insertion behavior.

1.1. Experimental conditions

As illustrated in figure 2, we designed single micro tube placed at the corner of a silicon sample in order to avoid unexpected contacts during the insertion. Indeed, parallelism

defects and bonding wire height could stop and compromise the single micro tube insertion. On the other side, some Al-Cu pad arrays are made on the edge of another silicon sample as illustrated in figure 3. Moreover, electrical circuits and bonding pads are added from the previous version in order to allow four wire electrical characterizations. In this study we work with micro tubes coated with a 240nm gold layer in thicknesses.

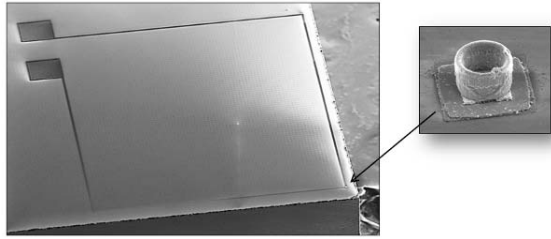


Fig. 2: Single micro tube isolated on a silicon substrate with electrical connection

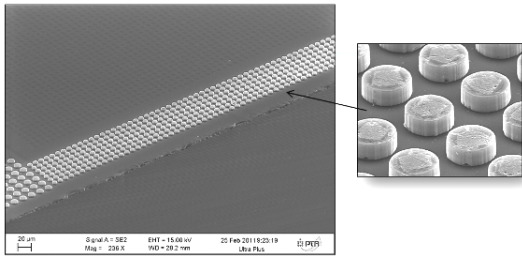


Fig. 3: Al-Cu pad arrays on the edge of a silicon substrate with electrical connections

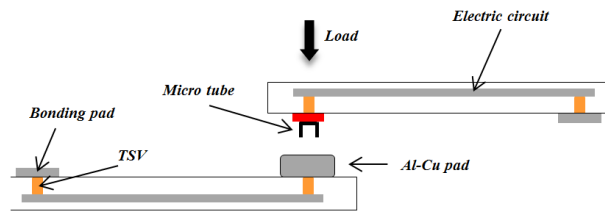


Fig. 4: Schematic drawing of single micro tube insertions

Mechanical characterizations were performed owing to a MTS XP nanoindenter, which principle was previously presented by M. Diop et al [6].

Using the micro tube as an indenter tip which is schematized in figure 4, we followed its insertion into $3\mu\text{m}$ high Al-Cu full sheet layer or pads with diameters of $4\mu\text{m}$ and $7\mu\text{m}$. The main objective of this first study is to determine the most efficient applied load to insert a micro tube as quickly as possible to answer to industrial requirements. Then, the strength of the connection is characterized by a vertical pull out test and the friction between the Al-Cu pillar and the micro tube can be quantified. In the present study, results will be given for $2.8\mu\text{m}$ high and $4\mu\text{m}$ diameter micro tubes. The micro tube's composition is proprietary but is considered as a hard material when compared to Al-0.5Cu pad. Also, all insertion experiments presented in this paper were performed at

different loading speed varying in $[300\mu\text{N/s}$ to $450\mu\text{N/s}]$ range.

An electrical measurement device is then added to carry out efficient and precise electromechanical insertion of a single micro tube. The main objective of this experiment is to study the evolution of the electrical contact during the micro tube insertion. The time and the micro tube insertion depth required to establish an acceptable electrical contact can be determined. Figure 5 schematizes the experimental set up used to achieve reliable electrical measurement. The nanoindenter is used to detect the contact between the micro tube and the Al-Cu pad. Then, a triggering signal is sent to the Source Measurement Unit (SMU). This signal allows synchronizing the beginning of the electrical measurement and the micro tube insertion into the pad.

To achieve mechanical and electromechanical experiments, the micro tube sample is glued on a specific support presented in figure 6 which allows electrical bonding and connection to Bayonet Neill-Concelman (BNC) connectors. Figure 7 illustrates the Al-Cu pad sample which is also glued on a specific pillar in order to ensure electrical bonding and connections to BNC connectors. Thanks to these two specific devices, the single micro tube is aligned above the Al-Cu pad. Then the micro tube is slowly getting closer to the Al-Cu pad and the nanoindenter detect the contact between them to send a triggering signal to the SMU. After that, the micro tube insertion and the electrical measurement are achieved. Finally, the electrical measurement is stopped when the micro tube is unloaded and a mechanical pull out test is carried out to characterize the strength of the assembly.

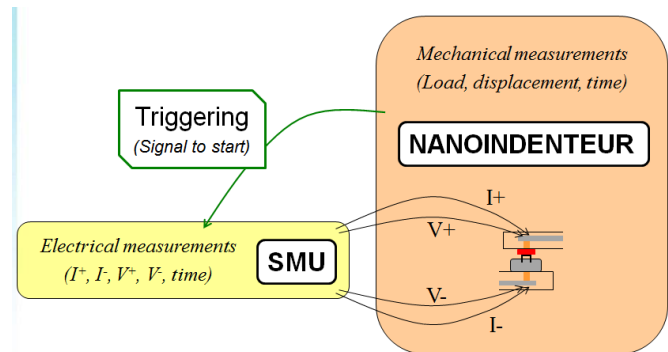


Fig. 5: Schematic drawing of the electromechanical measurement

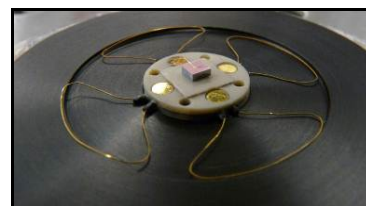


Fig. 6: Single micro tube sample glued and bonded on the specific support.

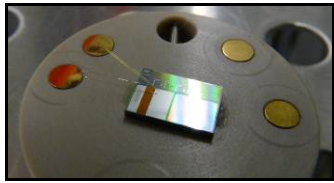


Fig. 7: Al-Cu pad sample glued and bonded on a specific pillar

1.2. Mechanical insertion characterization

Figure 8 shows typical load versus displacement curves recorded during the insertion of a single micro tube into a 3 μ m thick Al-Cu full sheet deposit. As illustrated in figure 9, all of these curves have been achieved at different position into the Al-Cu full sheet layer, the maximum load varying from 3800 μ N to 10500 μ N. It can be observed that this single micro tube insertion experiment is very repeatable and that the load required to insert the micro tube describes a bilinear behavior. The behavior variation point is observed around a 400nm insertion depth. Furthermore, the load required to pull out the micro tube increases with its insertion depth. This was expected, but the experiments allow us to determine the load required to pull out a full inserted micro tube. Thanks to that it is possible to estimate the pure vertical strength of a micro tube array assembly.

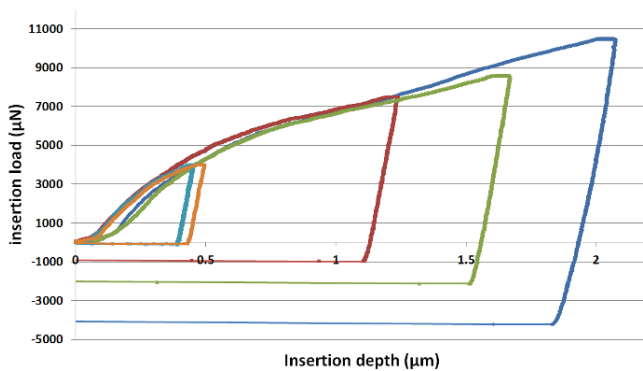


Fig. 8: Micro tube insertion into Al-Cu full sheet

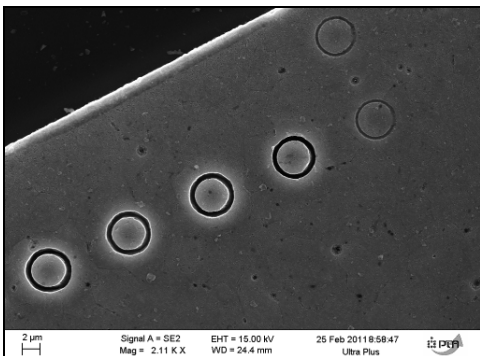


Fig. 9: Single micro tube insertion into Al-Cu full sheet layer

Then micro tube insertions were carried out using single micro tube into 3 μ m thick and 4 μ m in diameter Al-Cu pads. The objective of this experiment is to analyze the influence of the contact section on the insertion and on the pull out loads needed. In this study, the maximum insertion depth is fixed

and the load required to insert the micro tube is measured. As expected, the figure 10 shows that the insertion load decreases while the micro tube misalignment above the Al-Cu pad is increased. Indeed, such as illustrated in figure 11, the better is the micro tube alignment the bigger is the contact section between the micro tube and the pad.

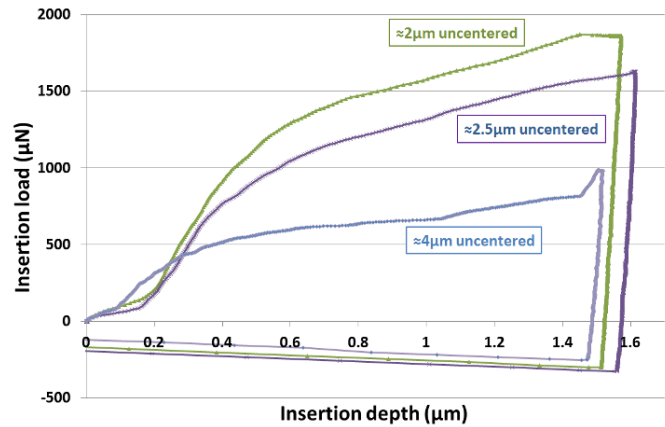


Fig. 10: Micro tube insertion into $\Phi 4\mu$ m Al-Cu pads

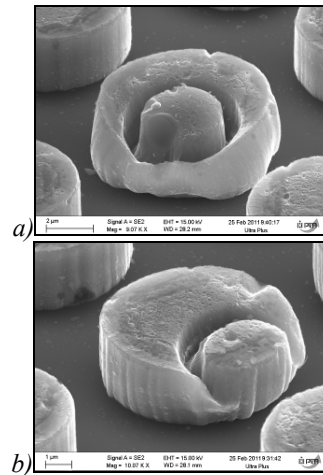


Fig. 11: a) Centered and b) not centered single micro tube insertion into $\Phi 7\mu$ m Al-cu pad

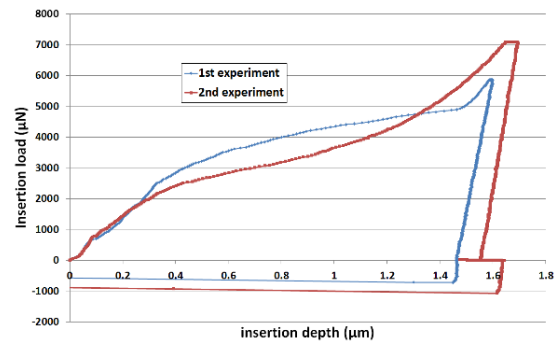


Fig. 12: Single micro tube insertion into $\Phi 7\mu$ m Al-Cu pad

1.3. Electromechanical insertion characterization

Figure 12 reports typical load versus displacement curves recorded during electromechanical single micro tube insertions into Al-Cu pads with a 3 μ m thickness and a

diameter of $7\mu\text{m}$. The loading rate of these experiments was equal to $300\mu\text{N/s}$ in order to be representative of D2W assemblies. Moreover, the micro tube was not fully inserted in order to avoid failure and to be able to pull out the micro tube. Electrical measurements are carried out by applying a differential potential of 10mV and by measuring currents from 10nA to 1A . In addition, the differential potential is alternatively positive and negative in order to remove electromotive forces.

Figure 13 shows electrical interconnection resistance versus micro tube insertion depth curves. It can be observed that the electrical resistance of the interconnection quickly decreases while the micro tube has reached a significant insertion depth. In these two experiments, the final electrical resistance obtained is approximately equal to $2.65\ \Omega$ and the insertion depth corresponds to 60% of the total tube height. Moreover, these measurements emphasize the reproducibility of the experience.

Figure 14 describes the electrical resistance and the insertion depth evolutions during the loading and the unloading times. As it can be noticed, the maximum insertion depth was reached in 25 seconds and the interconnection resistance became less than $4\ \Omega$ in less than 10 seconds which corresponds to a $1\mu\text{m}$ insertion depth of the micro tube.

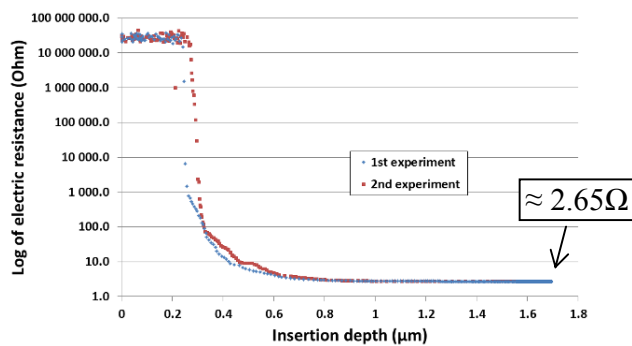


Fig. 13: Interconnection resistance regarding on the micro tube insertion depth

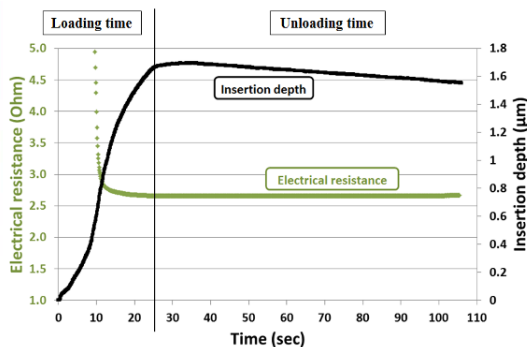


Fig. 14: Electromechanical measurement versus time

1.4. Analysis

First, figure 15 reports the load versus displacement curves recorded during the insertion of a single micro tube into either an Al-Cu full sheet layer of thickness $3\mu\text{m}$ or an Al-Cu pad of thickness $3\mu\text{m}$ and $7\mu\text{m}$ in diameter. It

confirms the substrate geometry has a strong influence on the insertion mechanics [7]. Moreover, the load required to fully insert a single micro tube into an Al-Cu pad is equal to 5.6mN . This value will be used for the design of experiment (DOE) used for D2W assemblies. Indeed, by extrapolating to 95000 interconnections, the load required to carry out D2W integrations would be equal to 530N .

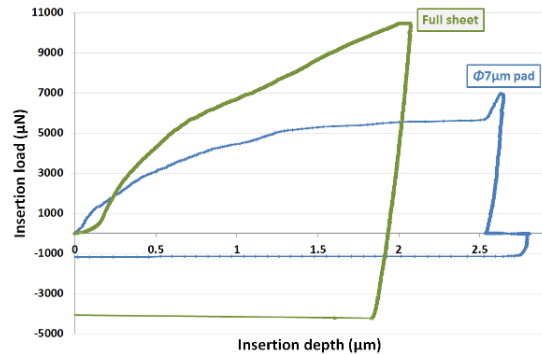


Fig. 15: Mechanical comparison into Al-Cu full sheet and pad

Pull-out analysis allowed to estimate the load required to remove a full inserted micro tube out of an Al-Cu pad. As illustrated in figure 16, the pull out load evolves quite linearly with the penetration depth when inserted into an Al-Cu full sheet layer. The curve slope obtained is approximately equal to $2500\mu\text{N}/\mu\text{m}$. More single micro tube insertions into Al-Cu pads are still required to confirm this value and to deduce the full inserted micro tube pull out load. Work is in progress to collect more data and to extrapolate to a D2W assembly with more than 95000 inserted micro tubes.

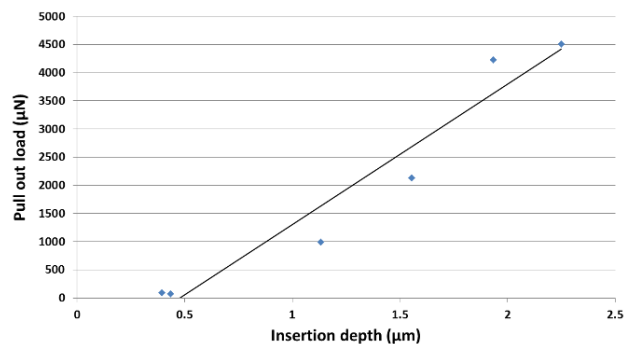


Fig. 16: pull out load required depending on the insertion depth into an Al-Cu full sheet layer

Concerning electromechanical measurements, we can observe in figure 13 and 14 that the electrical resistance decreases during the micro tube insertion. This confirms the electrical conduction along the micro tube walls while the micro tube insertion is become bigger than 300nm . This observation is important to deduce the maximum planarity and parallelism defects that the micro tube insertion technic can accommodate. In the present case, a $1\mu\text{m}$ insertion depth was sufficient to reach a vertical electrical resistance smaller than $3\ \Omega$. Therefore, a $1.5\mu\text{m}$ maximum planarity defects could be accommodated during D2W integration. Moreover, the holding time at maximum applied load does not

significantly influence the interconnection electrical resistance. Indeed, by unloading the micro tube, the assembly is relaxed and a negative displacement of 140 nm is measured. However, during this displacement, the electrical resistance increased of 10mΩ. This phenomenon could be due to a small displacement of the micro tube into the Al-Cu pad, added to elastic strain relaxation of the assembly. These observations will guide the experimental design used for D2W assembling in order to reduce the integration time and to be compatible with industrial requirements.

Finally, as illustrated in figure 17, the measured interconnection resistance R_{meas} , takes into account bonding resistance R_{tip} (tube in pad), via resistances R_{via} , and all layer interface resistances of the interconnection R_{int} such as

$$R_{meas} = 2R_{via} + R_{tip} + R_{int} \quad (1)$$

However, some homogeneity issues of via resistance have been observed depending on wafer location. That is why future work will be achieved to determine the pure bonding resistance R_{tip} value.

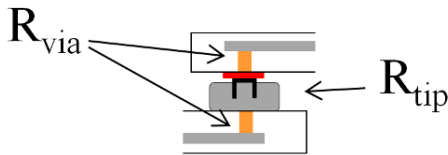


Fig. 17: interconnection resistance measurement

2. D2W Integration

The main objective of this part is to determine the best process parameters to carry out reliable D2W integrations taking into account industrial requirements. The previous single micro tube study is used to extrapolate to a chip with about 95000 interconnections. As illustrated in figure 18, an experimental design of 183 D2W hybridizations is carried out. The populated wafer is then electrically tested to validate our work and to determine which process parameters are the most significant.

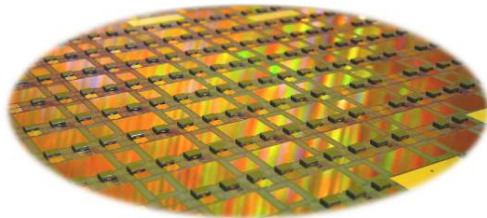


Fig 18: populated 200mm wafer with different insertion conditions (DOE)

2.1. Experimental conditions

As illustrated in figure 19, this work is achieved using dies constituted by cylindrical or star micro tubes. All of these micro tubes are 2.8μm high with diameters varying from 2μm to 4μm. Al-Cu pads presented in figure 20 are almost 3μm thick with a 7μm large square section.

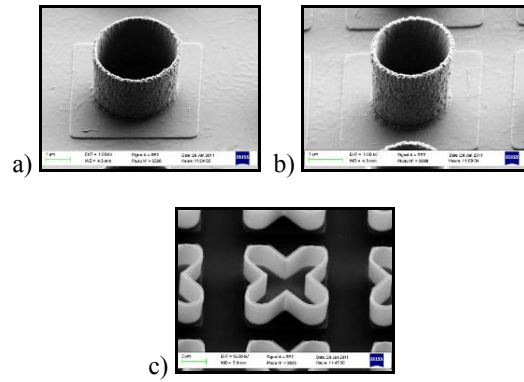


Fig 19: a) Φ4μm & b) Φ2μm micro tubes c) star tubes

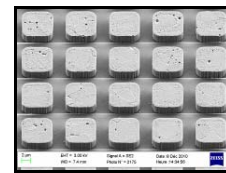


Fig 20: 7μm side square Al-Cu pad array

Bonding is performed thanks to an SET's FC300 flip-chip bonder. The assembly process is composed of a loading time followed by a holding pause at maximum load and an unloading time which can be modified for each test. The experimental design chosen for this study is based on a composed face centered cubic model with four replications of each point. As schematized in figure 21 and 22, we studied the influence of the maximum applied load F_M , the loading rate \dot{F} , the holding time t_h and the geometry of the micro tube on different responses. The integration time, the interconnection yield, the interconnection resistance and its standard deviation have been chosen as responses.

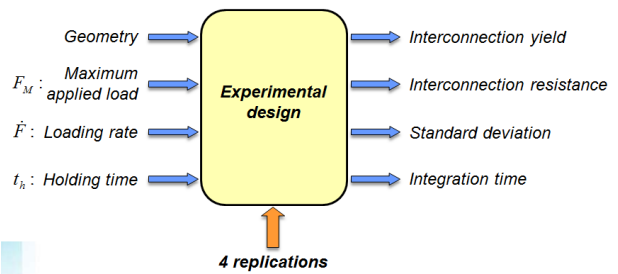


Fig 21: Experimental design used for D2W integrations

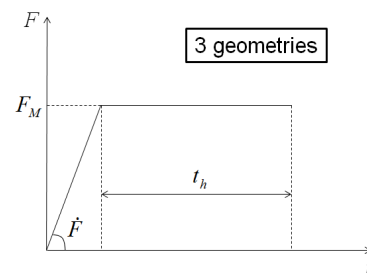


Fig 22: Schematized integration curve

2.2. Results

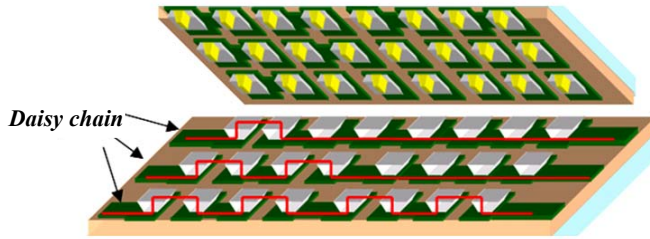


Fig 23: Daisy chain measurement principle

As schematized in figure 23, daisy chain resistance measurements are carried out on each D2W assembly in order to evaluate their electrical performance. The main objective is to evaluate the interconnection yield and the interconnection resistance depending on process parameters. This experimental design emphasizes that the more is the applied load the better are the interconnection resistance and the interconnection yield. However, the loading rate and the holding time used during the integration process do not significantly influence the interconnection performance. Thanks to these observations, integration parameters are chosen to reduce the bonding time and to improve the electrical performance and reliability. Table 2 summarizes the best input hybridization parameters used with $4\mu\text{m}$ in diameter micro tubes and table 3 presents mean corresponding results obtained. In this case, the 4 replications are used to analyze the result dispersion.

	Applied Load	Loading rate	Holding time	Load / μtube
$\Phi 4\mu\text{m}$ micro tube	400 N	50 N/sec	1 sec	4.2 mN

Table 2: typical parameters used with $\Phi 4\mu\text{m}$ micro tubes

	Interconnection		Insertion time
	Yield	Resistance	
$\Phi 4\mu\text{m}$ micro tube	99.15 %	3.23 Ω	9 sec.

Table 3: Average responses obtained with $\Phi 4\mu\text{m}$ micro tubes and table 2 parameters

The low yield result for this replicated experiment (99.15%) is attributed to one replication which is located at the periphery of the DOE wafer with defective via access. Additional experiments will be achieved to confirm those assumptions. Next, the average interconnection resistance equal to 3.23Ω is similar to the previous single micro tube analysis. First, these results confirm that the experimental set up used to study the single micro tube insertion behavior is suitable. Single micro tube insertions carried out thanks to the nanoindenter are directly transposable to flip-chip integration. Then, the integration time which represent the time needed to carry out a D2W integration can reach less than 10 seconds. This duration could be further reduced by increasing the loading rate and by removing the holding time at maximum load.

Finally, as future integration solution, micro tubes with a $2\mu\text{m}$ diameter and star tubes are analyzed. As summarized in table 4, both solutions present very good results regarding on interconnection performances and integration time. However, maximum load required to fully insert star tubes is higher than for cylindrical micro tubes. This explains the longer integration time needed to carry out full and reliable D2W hybridizations. Finally, some interconnection performance variations have been related to via resistance heterogeneities. This will be analyzed by taking into account the die integration location on the DOE wafer as an input parameter.

	Interconnection		Insertion time
	Yield	Resistance	
$\Phi 2\mu\text{m}$ micro tube	99.39 %	1.72 Ω	9 sec.
Star micro tube	100 %	2.52 Ω	18 sec.

Table 4: Average responses obtained with $\Phi 2\mu\text{m}$ micro tubes and star tubes

Conclusions and outlook

Single micro tube experimental study has confirmed the significant influence of the shape of the Al-0.5Cu pad. Thanks to this study the load required to fully insert a single micro tube into an Al-Cu pad has been determined to be equal to 5.6mN. Moreover, single electromechanical measurements have shown that a sufficient insertion depth is required to reach an efficient electrical contact. Indeed, the evolution of the electrical contact during the micro tube insertion shows a fast decreasing resistance after a 400nm depth. Then, the interconnection resistance is almost equal to 2.8 Ohms at $1.2\mu\text{m}$ insertion depth and reaches 2.65 at $1.6\mu\text{m}$. Further experiments will be carried out in order to reduce these values and some simulations will help to understand electrical resistance phenomena.

D2W assemblies have given interesting answers to industrial requirements with interconnection yield and resistance approximately equal to 99.15% and 3 Ohms respectively. As summarized in table 5, the load required to fully insert a single micro tube with diameter of $4\mu\text{m}$ into an Al-Cu pad of $7\mu\text{m}$ in diameter is equal to 5.6mN. Moreover, using a 50N/sec. loading rate, we determined a D2W bonding time of 9 seconds per die. This value could be improved by increasing this loading rate or by decreasing the micro tube diameter such as $2\mu\text{m}$ in diameter tubes. Then, thanks to micro tube wall conductivity, the electrical contact is established even if it is not fully inserted. That is why this technic can accommodate more than $1.5\mu\text{m}$ chip planarity defect while keeping good electrical contacts. Finally, all of these experiments have been achieved at room temperature and without the use of flux.

Finally, single electromechanical insertions and electrical simulations will be achieved in order to analyze the interconnection functioning. On wafer die location will be determined and used as a parameter to further analyze the experimental design followed. Maximum load applied on

dies built with 4µm in diameter micro tube will be increased in order to complete this work.

10 µm pitch	Yes?	Yes
Low assembling force	Yes	≈ 5.6mN/Interco.
Planarity compensation	Yes?	≈ 1.5µm
Room temperature	Yes	Yes
No flux used	Yes	Yes
Low D2W bonding time	Yes?	9sec. / die
Wafer To Wafer integration	No?	No?

Table 5: $\Phi 4\mu\text{m}$ micro tube capabilities results

Acknowledgments

This work was partly funded by the French Public Authorities through the NANO 2012 program. The authors would like to thank F. Berger, S. Lagarrigue, A. Bedoin, J. Routin, A. Gueugnot, I. Borel, J-M Debono, C. Poulain, R. Anciant, D. Mercier, F. De Crecy, D. Renaud, M. Rivoire, L. Vandroux and R. Boch from CEA-Leti, Minatec and K. Inal from the “Ecole Nationale supérieure des Mines de Saint-Etienne, Centre Microélectronique de Provence”. Moreover, this study has been achieved with the help of the “Laboratoire de Caractérisation et Fiabilité des Microsystèmes” of the CEA of Grenoble. Finally, this work has been performed with the help of the “Plateforme Technologique Amont” of Grenoble, with the financial support of the “Nanosciences aux limites de la Nanoélectronique” Foundation.

References

1. ITRS Road Map 2009 Edition Interconnect chapter.
2. P. Garrou, C. Bower, P. Ramm. Handbook of 3D integration: Technology and Applications of 3D Integrated Circuits. 2008 WILEY-VCH Verlag GmbH & Co. KGaA.
3. D. Saint-Patrice, F. Marion, M. Fendler et al. New Reflow Soldering and Tip in Buried Box (TB2) Techniques For Ultrafine Pitch Megapixels Imaging Array. *Proc 58th Electronic Components and Technology Conf*, Orlando, FL, 2008 p46-53.
4. F. Marion, D. Saint Patrice, M. Fendler et al. Electrical characterization of high count, 10 µm pitch, room-temperature vertical interconnections. Scottsdale az, march 2009.
5. M. Fendler, C. Davoine, F. Marion, D. Saint-Patrice, R. Fortunier, H. Ribot, “A fluxless and low-temperature flip chip process based on insertion technique,” *IEEE Trans-CPMT-A*, Vol. 32, No. 1 (2009), pp. 207-215.
6. M. Diop, V. Mandrillon et al. Analysis of nickel cylindrical bump insertion into aluminium thin film for flip chip applications. *Microelectronic Engineering* 87, 2010 p522–526
7. B. Goubault de Brugière, F. Marion, M. Fendler et al. Micro tube insertion into indium, copper and other materials for 3D applications. *Proc 60th Electronic Components and Technology Conf*, Las Vegas, NV, 2010 p1757-1762.

8. C. Okoro, R. Agarwal, P. Limaye et al. Insertion Bonding: A Novel Cu-Cu Bonding Approach for 3D Integration. *Proc 60th Electronic Components and Technology Conf*, Las Vegas, NV, 2010 p1370-1375.
9. N. Watanabe, T. Asano, Room-Temperature Chip-Stack Interconnection Using Compliant Bumps and Wedge-Incorporated Electrodes. *Proc 60th Electronic Components and Technology Conf*, Las Vegas, NV, 2010 p1763-1768.